Article:
Song, H, Huang, S, Jia, E et al. (3 more authors) (2020) Flat latitudinal diversity gradient caused by the Permian–Triassic mass extinction. Proceedings of the National Academy of Sciences of USA, 177 (30). pp. 17578-17583. ISSN 0027-8424

https://doi.org/10.1073/pnas.1918953117

Flat latitudinal diversity gradient caused by the Permian-Triassic mass extinction

Haijun Song[a]*, Shan Huang[b], Enhao Jia[a], Xu Dai[a], Paul B. Wignall[c], Alexander M. Dunhill[c]

[a]State Key Laboratory of Biogeology and Environmental Geology, School of Earth Science, China University of Geosciences, Wuhan 430074, China

[b]Senckenberg Biodiversity and Climate Research Center (SBiK-F), Senckenberganlage 25, 60325 Frankfurt (Main), Germany

[c]School of Earth and Environment, University of Leeds, Leeds LS2 9JT, UK

*Corresponding author. E-mail: haijunsong@cug.edu.cn

Significance

The deep time dynamics of the latitudinal diversity gradient (LDG), especially through dramatic events like mass extinctions, can provide invaluable insights on the biotic responses to global changes, yet they remain largely under-explored. Our study shows that the shape of marine LDGs changed substantially and rapidly during the Permian-Triassic mass extinction from a modern-like steep LDG to a flat LDG. The flat LDG lasted for ~5 million years and was likely a consequence of the extreme global environment, including extreme warming and ocean anoxia, which ensured harsh conditions prevailing from the tropics to the poles. Our findings highlight the fundamental role of environmental variations in concert with severe biodiversity loss in shaping the first-order biogeographic patterns.

Abstract:

The latitudinal diversity gradient (LDG) is recognized as one of the most pervasive, global patterns of present-day biodiversity. However, the controlling mechanisms have proved difficult to identify because many potential drivers covary in space. The geological record presents a unique opportunity for understanding the mechanisms which drive the LDG by providing a direct window to deep time biogeographic dynamics. Here we used a comprehensive database containing 52,318 occurrences of marine fossils to show that the shape of LDG changed greatly during the Permian-Triassic mass extinction from showing a significant tropical peak to a flattened LDG. The flat LDG lasted for the entire Early Triassic (~5 million years) before reverting to a modern-like shape in the Middle Triassic. The environmental extremes that prevailed globally, especially the dramatic warming, likely induced selective extinction in low latitudes and accumulation of diversity in high latitudes through origination and poleward migration, which combined together account for the flat LDG of the Early Triassic.

Keywords: biogeography | end-Permian mass extinction | global warming | ocean anoxia | biodiversity

The increase in species richness from the poles to the tropics, long known as the latitudinal diversity gradient (LDG), is one of the most pervasive first-order biological patterns on Earth today (1, 2), both on land (3) and in the oceans (4-6). Yet, the relative importance of the diverse ecological and evolutionary mechanisms (e.g., reviews in 7, 8, 9) for generating this pattern remains unclear. Paleontological data provide a unique perspective in the search for the dominant

driver(s) of LDGs, allowing diversity and distribution dynamics to be tracked through the long history of environmental changes (10, 11). In particular, climate (e.g., temperature or precipitation) is regarded as a key driver of the LDG, and its largescale changes have been postulated to have altered the general shape of the LDG through time (12, 13). Steep, normal LDGs (i.e., with a significant tropical peak like today) have been found primarily during icehouse times, whereas bimodal or even reverse LDGs with diversity peaks at mid- to high latitudes occurred during greenhouse climates (13, 14). These findings call for assessments of the relative importance of climate per se and environmental stability, especially through comparing the dynamics across several time intervals with different environmental templates.

The dramatic changes in environmental conditions and the severe mass extinction at the end of the Permian provide an excellent opportunity for investigating LDGs and their controlling mechanisms. The Permian-Triassic (P-Tr) mass extinction, which occurred *ca.* 252 million years ago, was the largest extinction event of the Phanerozoic (15, 16). This biological crisis was linked to extreme and prolonged environmental changes, many of which are probably the most serious of the past 500 million years. The contemporaneous eruption of the Siberian Traps large igneous province (17) drove ~10°C global warming within ca. 30,000-60,000 years through greenhouse gas emissions (18, 19), and widespread oceanic anoxia (20-22). These disastrous events killed over 90% of marine species (16), caused profound temporary and permanent ecological restructuring of marine ecosystems (23), which ultimately catalyzed the transformation of marine communities dominated by Paleozoic faunas to those dominated by the Modern fauna (15). The effect of the largest mass extinction in Earth history on global marine biogeography is largely unknown, but the rich marine fossil record from this time can be a powerful tool for illuminating the fundamental principles that shape global biodiversity.

LDG dynamics across the P-Tr mass extinction has received little attention except for a few case studies that have all suggested a strong impact of environmental changes on global diversity patterns. For example, the early-middle Permian diversity of terrestrial tetrapods reportedly peaked in temperate regions as a result of profound climate-induced biome shift (24). By the Early Triassic, the distribution of terrestrial tetrapods had moved 10–15° poleward (26, 27), and the group was apparently absent from 40°S to 30°N as a result of tropical overheating (18). Phylogenetic network analysis also found a marked increase in biogeographic connectedness, resulting in a more homogeneous composition of diversity across latitudes in tetrapods during this time (28). Similar poleward migrations were also found in marine invertebrates in the Northern Hemisphere during the Early Triassic (29), and a variable LDG during this time was reported in ammonoids (25). These findings suggest a great change in biogeographic distribution during the P-Tr crisis, which would have had a profound impact on LDG. In this study, we investigate LDG dynamics through the P-Tr mass extinction event, and the later recovery of biodiversity, using the most comprehensive fossil database thus far for this time period.

Global changes in biogeography

In order to assess the effect of the P-Tr extinction and associated environmental extremes on latitudinal diversity patterns, we analyzed biogeographic distributions using a new database consisting of occurrences of marine genera (including 20 major clades, see Methods for details) from the late Permian (Changhsingian - 254.1 Ma) to the Late Triassic (Rhaetian - 201.3 Ma). This database is an update of an earlier Permian-Triassic marine fossil database (23) and includes 52,318 generic occurrences at a substage- or stage-level resolution from 1768 literature sources (Database S1). Among these, 7,752, 12,676, 13,456, and 18,634 occurrences are in the late

93 Permian, Early, Middle, and Late Triassic, respectively. Based on reconstructed paleolatitudes,
94 the collections were binned into four paleolatitudinal zones for each hemisphere, i.e., 0–15°, 15–
95 30°, 30–45°, and 45–90°. The larger size of the 45–90° bin was chosen to accommodate the
96 relatively low sample density at higher latitudes in most time intervals. At the epoch level, data
97 from the paleolatitudinal zones of the northern and southern hemispheres are analyzed separately
98 (Fig. 1, *SI Appendix*, Fig. S1, Tables 1, 2). At stage/substage level, data from the northern and
99 southern hemispheres are amalgamated to ensure sufficient sample sizes (Fig. 2, *SI Appendix*,
100 Figs. S2–S4, Tables 3, 4). We standardized genus diversity in each paleolatitudinal zone for each
101 time bin using both incident-based rarefaction and extrapolation methods (see more details in
102 Methods).

103 We found the biodiversity peaks in the 30°N-15°S bins in both hot (Middle Triassic) and
104 cold (late Permian) times but a flatter LDG during the Early Triassic (Fig. 1), indicating a critical
105 role of environmental stability in maintaining a rich tropical fauna. Extrapolating diversity
106 estimators (Jackknife 1 and Chao 2, *SI Appendix*, Fig. S1*B*, *C*) show similar biogeographic
107 patterns with raw data for the four time intervals (*SI Appendix*, Fig. S1*A*). In the northern
108 hemisphere, genus diversity decreases from low to high paleolatitudes in the late Permian and
109 Middle Triassic. In the southern hemisphere, the 15-30° bin has the lowest diversity, which could
110 be partially explained by insufficient sample size (Fig. 1*A*). Most of southern hemisphere bins
111 from the late Permian and Middle Triassic intervals have generic occurrences of less than 380.
112 By contrast, both rarefied data and shareholder quorum subsampling (SQS) diversity show that
113 Early Triassic time bins were characterized by a nearly uniform genus richness from low to high
114 latitudes, except for the 45-90°N bin (Fig. 1). The low diversity in the 45-90°N bin is likely due
115 to a species-area effect (30), because this bin contained a smaller shelf area than other bins and

included an area of approximately half the shelf size compared to the 45-90°S bin during the Early Triassic (31). Additionally, there are more occurrences in the lower latitudes than there are in the mid and high latitudes for the Early Triassic (e.g., 6,057, 1,730, 3,788, and 1,101 occurrence records from low to high latitudes respectively), suggesting that the flat LDG is not a merely a sampling artifact. The Late Triassic interval is characterized by a diversity peak in the 15–30°N latitudinal bin, but exhibits a declining trend in diversity towards the polar region.

The raw data show slightly different LDG patterns in the late Permian and the Middle Triassic (*SI Appendix*, Fig. S1*A*), indicating that controlling for sampling variation is necessary for a rigorous investigation on fossil diversity patterns even with such a rich record. During the late Permian, 282 genera have been found from the regions in the 15–30°N zone, while 766 were found in the 0–15°N zone. Both rarefied and SQS diversities show less difference between the two latitude zones (Fig. 1), with the late Permian pattern more closely resembling the Middle Triassic pattern, implying a sampling effect in the raw data. Nevertheless, all subsampling methods have shown unmistakable flattening of LDG during the Early Triassic (Fig. 1), which provides compelling evidence for the strong impacts of mass extinction and dramatic environmental changes on global biogeography. Fossil data in the Early Triassic interval has a similar spatial distribution to other intervals (*SI Appendix*, Figs. S5, S6), suggesting that the flat LDG during the Early Triassic is not due to uneven spatial sampling and species-area effects (30).

Observed and estimated diversities at finer temporal resolution (i.e., 17 time bins including early Changhsingian, late Changhsingian, early Griesbachian, late Griesbachian, Dienerian, Smithian, Spathian, early Anisian, late Anisian, early Ladinian, late Ladinian, early Carnian, late Carnian, early Norian, middle Norian, late Norian, and Rhaetian) also show significant variations

of LDGs (Fig. 2, *SI Appendix*, Figs. S2–S4), i.e., from significant low latitude peaks in the late Permian to flat LDGs in the Early Triassic before returning back to LDGs with clear low latitude peaks in the Middle Triassic. Remarkably, diversity recovery occurred in all latitudes during the Smithian and Spathian intervals (late Early Triassic) and started in high latitudes, i.e., 30–90° zones (Fig. 2). The mid-latitude peak in observed diversity during the Carnian (*SI Appendix*, Fig. S2) is not entirely an artifact of sampling, because subsampled data also show a similar, but weaker peak (Fig. 2). In addition, the end-Norian marine biota experienced a short-term change in LDG, with lower diversity in the 0–15° zone than mid-latitude regions (Fig. 2, *SI Appendix*, Figs. S2–S4).

Drivers of the dynamic latitudinal diversity gradient

The similar LDGs during the hot Middle Triassic and cold late Permian contradict the notion that icehouse climates, which can maintain strong environmental gradients across space, are necessary to produce such LDGs (13). Previous studies have generally associated steep, normal LDG patterns with icehouse climates, such as the late Cenozoic including the present-day (5, 32-34), late Paleozoic (35), and late Ordovician (36, 37), suggesting a negative relationship between global temperature and the strength of LDG (13), albeit with some clade-specific exceptions (38). The late Permian (Changhsingian Stage) was a cold period, during which the temperature was only slightly higher than during the late Paleozoic glaciation (39); the strength of Changhsingian LDG is similar to the late Cenozoic LDG for marine animals with markedly elevated generic richness in the tropics (32). However, the Middle Triassic is commonly classified as a hothouse period with the average sea surface temperature ~8°C higher than seen at the present-day (40), and yet the steepness of LDG increased after the re-establishment of

environmental stability. The flattened shape of Early Triassic LDG matches well with ecological diversity data, which showed that the tropics had the highest level of functional diversity during the late Permian, but following the extinction, a similar level of functional diversity as higher latitudes (41).

In contrast to the global environment before and after this period, the dramatic environmental changes that began in the P-Tr boundary interval and lasted for ~ 5 million years are likely the leading causes of the lack of a discernable LDG in Early Triassic marine biota. These changes have three notable features:

(i) Strong intensity. Climatic/environmental conditions were the most severe of the past 500 million years, e.g., ~10°C increase of sea surface temperature in ca. 30,000-60,000 years (18, 19), rapid shifts between oxia and anoxia in shallow-waters (21), and a significant increase of continental weathering rates and nutrient delivery to the oceans (42, 43).

(ii) Global reach. Some environmental events, including anoxia and warming, affected most habitats and regions (21, 22, 44).

(iii) Frequent recurrence. Extreme warming, oceanic anoxia, and enhanced weathering occurred recurrently and such conditions lasted for the entire Early Triassic, ca. 5 million years (18, 20, 42, 43) (Fig. 4). Together, these unstable environmental conditions prevented diversity recovery, even in the tropics, and destroyed the advantage of this region as both the cradle and the museum for global biodiversity (45).

Under the stress of such extreme environment during the P-Tr crisis, preferential extinction at low latitudes may have played an important role in the transformation of LDGs. To evaluate this mechanism, we selected the Changhsingian and early Griesbachian as the interval to calculate extinction magnitude because the major extinction pulses straddled the P-Tr boundary (46). The

extinction magnitudes (calculated by the number of extinct genera/the number of total genera) in the Changhsingian and early Griesbachian interval are 78.7% and 72.4% in the 0–15° and 15–30° zones, respectively, which are higher than the 30–45° zone with extinction rates of 60.9% but not the 45–90° zone with 72.8% taxa extinct (Fig. 3B, *SI Appendix*, Table. S5). Other studies have suggested that the Changhsingian has a peak extinction in the higher latitudes, which is not seen in our data, but the Induan (Griesbachian and Dienerian) shows higher extinction in the tropics than temperate regions (22, 47), which better agrees with our work. A similar flat LDG pattern has also been found in mammals after the Cretaceous/Paleogene extinction event (48).

In addition, our results show higher origination and invasion rates at high latitudes in the late Griesbachian-Smithian interval (Fig. 3C), suggesting that high latitude regions had become the refuge and cradle for marine organisms after the P-Tr mass extinction. The higher invasion rates toward high latitudes (Fig. 3C) are also consistent with the expectation of a pervasive tendency of migrating poleward. Therefore, both higher diversification rates at high latitudes and poleward migration would have played significant roles in producing the flat LDG in the Early Triassic.

Our findings of a temporally dynamic LDG in response to environmental changes coincident with the P-Tr mass extinction is clear evidence for a strong role of major environmental crises and massive climate perturbations in producing flatter LDGs. For example, the delay of metazoan reef recovery in the Early Triassic was an important factor in suppressed equatorial diversity (49, 50) (Fig. 4), leading to a flatter LDG. Stable environments allow diversity to accumulate with higher speciation rates and/or lower extinction rates (51). However, because environmental stability and many other factors, especially climatic conditions, all co-vary with latitude, their relative importance in shaping the LDG are difficult to compare based on spatial analyses alone.

Unstable and harsh environments and the major loss of species during the P-Tr extinction resulted in unstable global communities (52), and weak biotic interactions in both low- and high-latitude regions. The blooms of opportunists (e.g., small foraminifers, linguloid brachiopods, microgastropods, and *Claraia* bivalves) in the aftermath of the P-Tr extinction (23, 53-55) indicate that r-strategists dominated the marine realm. Despite an apparent lack of selection for larger geographic range sizes during the P-Tr mass extinction (56), biogeographic cosmopolitanism increased in both terrestrial (28) and marine (25) realms in the Early Triassic, likely because surviving opportunistic taxa were able to proliferate geographically in the absence of intense competition and their larger niche breadths allowed them to cope with harsh and variable conditions.

The hothouse climates during the Early Triassic probably also contributed to weakening the marine LDG. Sea surface temperature of low-latitudes in the Early Triassic was ~15°C higher than at present (40). An Earth system model of P-Tr climate suggests that the amplitude of warming in high-paleolatitudes is much higher than that in low-paleolatitudes (22), resulting in a weak latitudinal temperature gradient. Additionally, extreme seawater temperatures (up to 35 °C), and associated anoxia would have been lethal to many tropical organisms (Fig. 4). An analog is happening in modern oceans, i.e., the declining oxygen caused by global warming and eutrophication is influencing marine life from gene to ecosystem levels (57).

Global temperatures declined by ~4 °C in the early Middle Triassic when compared to the Early Triassic hothouse (18), which may have been enough to facilitate the re-establishment of a normal LDG in the mid-Triassic. Our findings suggest that only extreme and variable hothouse climates produce flat LDGs while a stable greenhouse world can still have enough pole to equator climatic gradient to produce a significant, normal LDG. Among other factors, the yearly

seasonal instability, including the variation of solar radiation and daylight, is likely a major cause of lower biodiversity at higher latitudes even during greenhouse periods.

Causes of Late Triassic biogeographic changes

During the Late Triassic, marine organisms were most diverse in the 15-30°N region (Fig. 1). A mid-latitude peak of marine biodiversity has been reported in modern taxa (14), post-Paleozoic brachiopods (58), and Early and Middle Ordovician taxa (37). Temperature and shelf areas have been proposed as the primary variables influencing the bimodality of LDG (14, 37, 59). High temperatures in tropics are beyond the thermal optima for some taxa, especially during global warming intervals. Paleogeographic data show shelf area increased remarkably in the mid-latitudes of the northern hemisphere during the Late Triassic (31), which would have provided more habitats for marine organisms and accordingly contributed to higher diversity.

The mid-latitude peak in diversity during the Carnian is probably due to extreme climate events that happened in the mid-Carnian interval. Carbon isotope records show a major negative excursion in both organic and carbonate $\delta^{13}C$ at this time (60, 61), reflecting significant perturbations of the carbon cycle. Sea surface temperature increased about 6°C in this interval (62, 63), which coincided with the major negative shift of $\delta^{13}C$ (63), suggesting a causal linkage between the injection of pCO_2 and global warming. The mid-Carnian event also affected the marine biota and resulted in a biodiversity decline (23) and some ecological changes (64).

The drop of diversity in the low latitudes during the end-Norian interval is probably associated with environmental disturbance (62, 65). Conodont oxygen isotope data suggested a ~7°C warming in the late Norian, which lasted about 7 million years (62). Significant negative

excursions of organic carbon and nitrogen isotope ratios near the Norian-Rhaetian boundary suggest the development of widespread oceanic stagnation during this interval (65).

Implications for modern ecosystem changes

Identifying the main drivers of global biogeographic patterns is a critical step towards predicting future responses to projected environmental changes. In particular, our results support the previous suggestion that extreme climatic events, particularly when combined with other anthropogenic effects, will lead to severe consequences for biodiversity (57), although a super greenhouse Triassic-like world is a distant and perhaps unlikely prospect. We show a flattening of the LDG after the biggest mass extinction, which indicates a collapse of tropical ecosystems including tropical reefs. We already know that modern reefs are highly stressed (66, 67) and it seems that they will likely be the first major victims of warming and, given that these are the most diverse of all marine ecosystems, this will contribute to a flattening of the modern marine LDG (66, 68).

Methods

Fossil database. We substantially updated an earlier database of Permian-Triassic marine fossils (23) by adding 89 publications for 1263 fossil occurrences including data from the Paleobiology Database (PBDB). Fossil occurrences were compiled for 17 substage-/stage-level time bins, following GSA Geological Time Scale v. 5.0 (69), from the late Permian Changhsingian (starting 254.1 Ma) to the Late Triassic Rhaetian (ending 201.3 Ma), including, in sequential order, early Changhsingian, late Changhsingian, early Griesbachian, late Griesbachian, Dienerian, Smithian, Spathian, early Anisian, late Anisian, early Ladinian, late Ladinian, early Carnian, late Carnian, early Norian, middle Norian, late Norian, and Rhaetian. The taxonomy and biostratigraphy were

277 rigorously validated to ensure consistency across the database. We based our analyses on genus-
278 level occurrences because species-level identification is often inaccurate and spotty.
279 The resulting new global fossil database contains 52,318 generic occurrences from 4,875
280 collections in 1,768 publications (see Database S1). The total 4,342 genera belong to 20 major
281 groups including three clades of algae (benthic calcareous algae, coccoliths, and dinoflagellates),
282 two clades of protozoa (foraminifers and radiolarians), twelve clades of invertebrates (annelids,
283 bivalves, brachiopods, bryozoans, cephalopods, corals, echinoderms, gastropods, hydrozoans,
284 ostracods, non-ostracod crustaceans, and sponges), and three clades of vertebrates (conodonts,
285 fishes, and marine reptiles).
286
287 **Paleolatitude reconstruction.** Paleolatitudes (and paleolongitudes) were reconstructed using
288 PointTracker v7 rotation files published by the PALEOMAP Project (70) based upon the
289 present-day georeference data and a model of global tectonic history. Paleolatitude data were
290 reconstructed for every 10 million years, e.g., with mid-points at 250 Ma for time bins from
291 Changhsingian to early Anisian; 240 Ma for late Anisian and Ladinian; 230 Ma for Carnian, 220
292 Ma for early and middle Norian; 210 Ma for late Norian and Rhaetian.
293 The fossil occurrences for each time bin were grouped into four paleolatitudinal zones in
294 each hemisphere, i.e., 0°–15°, 15°–30°, 30°–45°, and 45°–90°. The high-latitude zone covers a
295 total of 45 degrees of latitudes because the sample sizes for 15-degree regions at high latitudes in
296 most time bins were insufficient for rigorous analyses of diversity patterns. However, we note
297 that higher latitudinal bands tend to cover smaller geographic areas than lower bands of the same
298 number of degrees, which reduces the issue of uneven sampling areas. Further, we employed
299 statistical methods to account for the sampling effects across latitudinal zones. Spanning the

whole focal period in our study, the four paleolatitudinal zones contained a total of 22,526, 13,649, 11,571, and 4,572 occurrences, respectively, from low to high latitudes.

Rarefaction method. We applied the rarefaction method to compare generic richness across latitudinal zones and time bins (71, 72), using the program PAleontological STatistics (PAST, Version 3.16) (73). Because our dataset includes both micro- and macrofossil groups that systematically differ in the abundance of individuals in each collection (23), abundance does not make an appropriate unit for the subsampling procedures for comparing total marine diversity. Instead, we treated each generic occurrence (the unique stratigraphic unit in which this genus occurred) as an individual sampling unit, which serves as the analytical unit for rarefaction. We randomly subsampled the fossil occurrences from each latitudinal zone in each time bin until a specific quota based on the minimum sample size in latitudinal pools. We generated rarefaction curves in two temporal resolutions to compare LDGs, i.e., in the four epochs (the late Permian, Early, Middle, and Late Triassic) and in the more refined 17 time bins as explained above. The latitudinal faunas in each epoch were rarefied using a quota of 380. The fossil occurrences in the 17 time bins were subsampled until a quota of 136 occurrences in each latitudinal zone.

SQS method. Shareholder quorum subsampling (SQS) approach (74) was applied to estimate diversity variation across latitudes in the late Permian, Early, Middle, and Late Triassic intervals. SQS diversities were calculated with the divDyn R package at a quorum level of 0.5 (75).

Data access and availability. All data used to conduct analyses and plot figures are available for download at https://doi.org/10.5061/dryad.41ns1rn9z.

ACKNOWLEDGMENTS.

We thank the contributors to the Paleobiology Database and Philip Mannion and two anonymous reviewers for constructive reviews. This is Paleobiology Database publication number xxx. This research was supported by the National Natural Science Foundation of China (41821001), the State Key R&D project of China (2016YFA0601100), the Strategic Priority Research Program of Chinese Academy of Sciences (XDB26000000), a Marie Curie Fellowship (H2020-MSCA-IF-2015-701652), the Natural Environment Research Council (NE/P0137224/1), and the German Science Foundation (DFG, HU 2748/1-1).

Author contributions: H.S., P.B.W., A.M.D. conceived the study. H.S. and E.J. collected fossil data. H.S., S.H., and X.D. carried out the data analysis. H.S., S.H., P.B.W, and A.M.D. wrote the paper. All authors contributed to data interpretation and the writing of the manuscript.

The authors declare that they have no competing interests.

References

1. Pianka ER (1966) Latitudinal gradients in species diversity: a review of concepts. *Am Nat* 100(910):33–46.
2. Hillebrand H (2004) On the generality of the latitudinal diversity gradient. *Am Nat* 163(2):192–211.
3. Willig MR, Kaufman DM, & Stevens R (2003) Latitudinal gradients of biodiversity: pattern, process, scale, and synthesis. *Annu Rev Ecol Evol Syst* 34(1):273–309.
4. Roy K, Jablonski D, Valentine JW, & Rosenberg G (1998) Marine latitudinal diversity gradients: tests of causal hypotheses. *Proc Natl Acad Sci USA* 95(7):3699–3702.
5. Huang S, Roy K, Valentine JW, & Jablonski D (2015) Convergence, divergence, and parallelism in marine biodiversity trends: Integrating present-day and fossil data. *Proc Natl Acad Sci USA* 112(16):4903–4908.
6. Yasuhara M, Hunt G, Dowsett HJ, Robinson MM, & Stoll DK (2012) Latitudinal species diversity gradient of marine zooplankton for the last three million years. *Ecol Lett* 15(10):1174–1179.

7. Mittelbach GG*, et al.* (2007) Evolution and the latitudinal diversity gradient: speciation, extinction and biogeography. *Ecol Lett* 10(4):315–331.
8. Jablonski D, Huang S, Roy K, & Valentine JW (2017) Shaping the latitudinal diversity gradient: new perspectives from a synthesis of paleobiology and biogeography. *Am Nat* 189(1):1–12.
9. Fine PV (2015) Ecological and evolutionary drivers of geographic variation in species diversity. *Annu Rev Ecol Evol Syst* 46:369–392.
10. Yasuhara M, Hunt G, Cronin TM, & Okahashi H (2009) Temporal latitudinal-gradient dynamics and tropical instability of deep-sea species diversity. *Proc Natl Acad Sci USA* 106(51):21717–21720.
11. Yasuhara M, Tittensor DP, Hillebrand H, & Worm B (2017) Combining marine macroecology and palaeoecology in understanding biodiversity: microfossils as a model. *Biol Rev* 92(1):199–215.
12. Saupe EE*, et al.* (2019) Non‐random latitudinal gradients in range size and niche breadth predicted by spatial patterns of climate. *Global Ecol Biogeogr* 28(7):928–942.
13. Mannion PD, Upchurch P, Benson RBJ, & Goswami A (2014) The latitudinal biodiversity gradient through deep time. *Trends Ecol Evol* 29(1):42–50.
14. Chaudhary C, Saeedi H, & Costello MJ (2016) Bimodality of latitudinal gradients in marine species richness. *Trends Ecol Evol* 31(9):670–676.
15. Sepkoski JJ, Jr (1984) A kinetic model of Phanerozoic taxonomic diversity, III. Post-Paleozoic families and mass extinctions. *Paleobiology* 10(2):246–267.
16. Erwin DH (1994) The Permo-Triassic extinction. *Nature* 367:231–236.
17. Bond DP & Wignall PB (2014) Large igneous provinces and mass extinctions: an update. *Geol Soc Am Spec Pap* 505:SPE505–502.
18. Sun Y*, et al.* (2012) Lethally hot temperatures during the Early Triassic greenhouse. *Science* 338(6105):366–370.
19. Shen S-Z*, et al.* (2018) A sudden end-Permian mass extinction in South China. *Geol Soc Am Bull* 131(1-2):205–223.
20. Song H*, et al.* (2012) Geochemical evidence from bio-apatite for multiple oceanic anoxic events during Permian–Triassic transition and the link with end-Permian extinction and recovery. *Earth Planet Sci Lett* 353–354:12–21.
21. Wignall PB*, et al.* (2016) Ultra-shallow-marine anoxia in an Early Triassic shallow-marine clastic ramp (Spitsbergen) and the suppression of benthic radiation. *Geol Mag* 153(2):316–331.
22. Penn JL, Deutsch C, Payne JL, & Sperling EA (2018) Temperature-dependent hypoxia explains biogeography and severity of end-Permian marine mass extinction. *Science* 362(6419):eaat1327.
23. Song H, Wignall PB, & Dunhill AM (2018) Decoupled taxonomic and ecological recoveries from the Permo-Triassic extinction. *Sci Adv* 4(10):eaat5091.
24. Brocklehurst N, Day MO, Rubidge BS, & Fröbisch J (2017) Olson's extinction and the latitudinal biodiversity

gradient of tetrapods in the Permian. *Proc R Soc B Biol Sci* 284(1852):20170231.

25. Brayard A*, et al.* (2006) The Early Triassic ammonoid recovery: Paleoclimatic significance of diversity gradients. *Palaeogeogr, Palaeoclimatol, Palaeoecol* 239(3–4):374–395.

26. Bernardi M, Petti Fabio M, & Benton Michael J (2018) Tetrapod distribution and temperature rise during the Permian–Triassic mass extinction. *Proc R Soc B Biol Sci* 285(1870):20172331.

27. Benton MJ (2018) Hyperthermal-driven mass extinctions: killing models during the Permian–Triassic mass extinction. *Philos Trans R Soc A* 376(2130):20170076.

28. Button DJ, Lloyd GT, Ezcurra MD, & Butler RJ (2017) Mass extinctions drove increased global faunal cosmopolitanism on the supercontinent Pangaea. *Nat Comm* 8(1):733.

29. Reddin CJ, Kocsis ÁT, & Kiessling W (2018) Marine invertebrate migrations trace climate change over 450 million years. *Global Ecol Biogeogr* 27(6):704–713.

30. Close RA, Benson RB, Upchurch P, & Butler RJ (2017) Controlling for the species-area effect supports constrained long-term Mesozoic terrestrial vertebrate diversification. *Nat Comm* 8(1):15381.

31. Scotese CR (2014) Atlas of Permo-Triassic paleogeographic maps,(mollweide projection). *PALEOMAP Atlas for ArcGIS* 3–4:43–52.

32. Alroy J*, et al.* (2008) Phanerozoic trends in the global diversity of marine invertebrates. *Science* 321(5885):97–100.

33. Jablonski D, Roy K, & Valentine JW (2006) Out of the tropics: Evolutionary dynamics of the latitudinal diversity gradient. *Science* 314(5796):102–106.

34. Miraldo A*, et al.* (2016) An Anthropocene map of genetic diversity. *Science* 353(6307):1532–1535.

35. Powell MG (2005) Climatic basis for sluggish macroevolution during the late Paleozoic ice age. *Geology* 33(5):381–384.

36. Krug AZ & Patzkowsky ME (2007) Geographic variation in turnover and recovery from the Late Ordovician mass extinction. *Paleobiology* 33(3):435–454.

37. Kröger B (2017) Changes in the latitudinal diversity gradient during the Great Ordovician Biodiversification Event. *Geology* 46(2):127–130.

38. Mannion PD*, et al.* (2015) Climate constrains the evolutionary history and biodiversity of crocodylians. *Nat Comm* 6(1):9438.

39. Chen B*, et al.* (2013) Permian ice volume and palaeoclimate history: Oxygen isotope proxies revisited. *Gondwana Res* 24(1):77–89.

40. Song H, Wignall PB, Song H, Dai X, & Chu D (2019) Seawater temperature and dissolved oxygen over the past 500 million years. *J Earth Sci* 30(2):236–243.

41. Foster WJ & Twitchett RJ (2014) Functional diversity of marine ecosystems after the Late Permian mass extinction event. *Nat Geosci* 7(1):233–238.

42. Algeo TJ & Twitchett RJ (2010) Anomalous Early Triassic sediment fluxes due to elevated weathering rates

and their biological consequences. *Geology* 38(11):1023–1026.

43. Song H*, et al.* (2015) Integrated Sr isotope variations and global environmental changes through the Late Permian to early Late Triassic. *Earth Planet Sci Lett* 424:140–147.

44. Grasby S, Beauchamp B, Embry A, & Sanei H (2013) Recurrent Early Triassic ocean anoxia. *Geology* 41(2):175–178.

45. Jablonski D*, et al.* (2013) Out of the tropics, but how? Fossils, bridge species, and thermal ranges in the dynamics of the marine latitudinal diversity gradient. *Proc Natl Acad Sci USA* 110(26):10487–10494.

46. Song H, Wignall PB, Tong J, & Yin H (2013) Two pulses of extinction during the Permian-Triassic crisis. *Nat Geosci* 6(1):52–56.

47. Reddin CJ, Kocsis ÁT, & Kiessling W (2019) Climate change and the latitudinal selectivity of ancient marine extinctions. *Paleobiology* 45(1):70–84.

48. Rose PJ, Fox DL, Marcot J, & Badgley C (2011) Flat latitudinal gradient in Paleocene mammal richness suggests decoupling of climate and biodiversity. *Geology* 39(2):163–166.

49. Flügel E (2002) Triassic reef patterns. *Phanerozoic reef patterns,* Special Publication - Society for Sedimentary Geology, 72, eds Kiessling W, Flügel E, & Golonka J (Society for Sedimentary Geology (SEPM), Tulsa), pp 391–463.

50. Kiessling W (2010) Reef expansion during the Triassic: Spread of photosymbiosis balancing climatic cooling. *Palaeogeogr, Palaeoclimatol, Palaeoecol* 290(1–4):11–19.

51. Pontarp M*, et al.* (2019) The latitudinal diversity gradient: Novel understanding through mechanistic eco-evolutionary models. *Trends Ecol Evol* 34(3):211–223.

52. Roopnarine PD & Angielczyk KD (2015) Community stability and selective extinction during the Permian-Triassic mass extinction. *Science* 350(6256):90–93.

53. Peng Y, Shi GR, Gao Y, He W, & Shen S (2007) How and why did the Lingulidae (Brachiopoda) not only survive the end-Permian mass extinction but also thrive in its aftermath? *Palaeogeogr, Palaeoclimatol, Palaeoecol* 252(1–2):118–131.

54. Fraiser ML & Bottjer DJ (2004) The non-actualistic Early Triassic gastropod fauna: a case study of the Lower Triassic Sinbad Limestone Member. *Palaios* 19(3):259–275.

55. Petsios E & Bottjer DJ (2016) Quantitative analysis of the ecological dominance of benthic disaster taxa in the aftermath of the end-Permian mass extinction. *Paleobiology* 42(3):380–393.

56. Harnik Paul G, Simpson C, & Payne JL (2012) Long-term differences in extinction risk among the seven forms of rarity. *Proc R Soc B Biol Sci* 279(1749):4969–4976.

57. Breitburg D*, et al.* (2018) Declining oxygen in the global ocean and coastal waters. *Science* 359(6371):eaam7240.

58. Powell MG, Moore BR, & Smith TJ (2015) Origination, extinction, invasion, and extirpation components of the brachiopod latitudinal biodiversity gradient through the Phanerozoic Eon. *Paleobiology* 41(2):330–341.

59. Saeedi H, Dennis TE, & Costello MJ (2017) Bimodal latitudinal species richness and high endemicity of razor clams (Mollusca). *J Biogeogr* 44(3):592–604.

60. Dal Corso J*, et al.* (2012) Discovery of a major negative $\delta^{13}C$ spike in the Carnian (Late Triassic) linked to the eruption of Wrangellia flood basalts. *Geology* 40(1):79–82.

61. Mueller S, Krystyn L, & Kürschner WM (2016) Climate variability during the Carnian Pluvial Phase — A quantitative palynological study of the Carnian sedimentary succession at Lunz am See, Northern Calcareous Alps, Austria. *Palaeogeogr, Palaeoclimatol, Palaeoecol* 441:198–211.

62. Trotter JA, Williams IS, Nicora A, Mazza M, & Rigo M (2015) Long-term cycles of Triassic climate change: a new δ18O record from conodont apatite. *Earth Planet Sci Lett* 415(0):165–174.

63. Sun YD*, et al.* (2016) Climate warming, euxinia and carbon isotope perturbations during the Carnian (Triassic) Crisis in South China. *Earth Planet Sci Lett* 444:88–100.

64. Dunhill AM, Foster WJ, Sciberras J, & Twitchett RJ (2018) Impact of the Late Triassic mass extinction on functional diversity and composition of marine ecosystems. *Palaeontology* 61(1):133–148.

65. Sephton MA*, et al.* (2002) Carbon and nitrogen isotope disturbances and an end-Norian (Late Triassic) extinction event. *Geology* 30(12):1119–1122.

66. Hughes TP*, et al.* (2017) Global warming and recurrent mass bleaching of corals. *Nature* 543:373–377.

67. De'ath G, Lough JM, & Fabricius KE (2009) Declining coral calcification on the Great Barrier Reef. *Science* 323(5910):116–119.

68. Harborne AR, Rogers A, Bozec Y-M, & Mumby PJ (2017) Multiple stressors and the functioning of coral reefs. *Ann Rev Mar Sci* 9(1):445–468.

69. Walker J, Geissman J, Bowring S, & Babcock L (2018) *GSA Geological Time Scale v. 5.0* (Geological Society of America).

70. Scotese C (2008) The PALEOMAP Project PaleoAtlas for ArcGIS. (PALEOMAP Project, Arlington, Texas).

71. Miller AI & Foote M (1996) Calibrating the Ordovician radiation of marine life: implications for Phanerozoic diversity trends. *Paleobiology* 22(02):304–309.

72. Alroy J*, et al.* (2001) Effects of sampling standardization on estimates of Phanerozoic marine diversification. *Proc Natl Acad Sci USA* 98(11):6261–6266.

73. Hammer Ø, Harper D, & Ryan P (2017) *PAST: paleontological statistics. Version 3.16* (National History Museum, University of Oslo) p 256.

74. Alroy J (2010) Fair sampling of taxonomic richness and unbiased estimation of origination and extinction rates. *Paleontol Soc Pap* 16:55–80.

75. Kocsis AT, Reddin CJ, Alroy J, & Kiessling W (2019) The R package divDyn for quantifying diversity dynamics using fossil sampling data. *Methods Ecol Evol* 10(5):735–743.

Figure captions

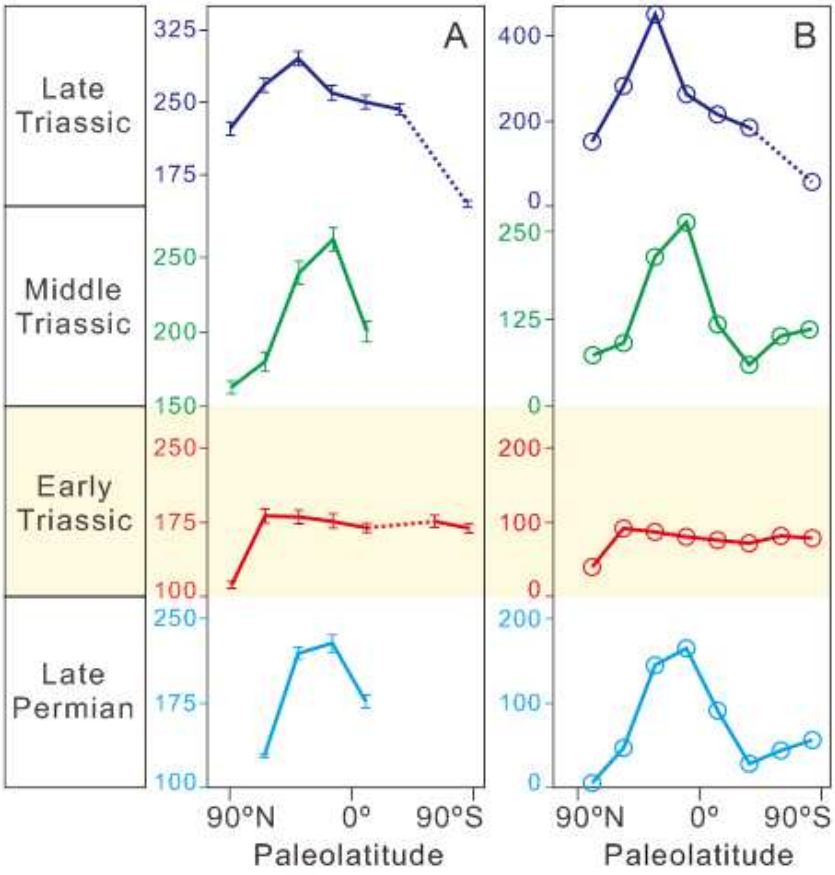

Fig. 1. Latitudinal diversity gradients for late Permian and Triassic intervals. (*A*) Subsampled diversity using a quota of 380 occurrences for each time interval. Vertical bar presents the standard deviation. (*B*) Shareholder quorum subsampling (SQS) diversity with a quorum level of 0.5. Dash line represents the discontinuous case.

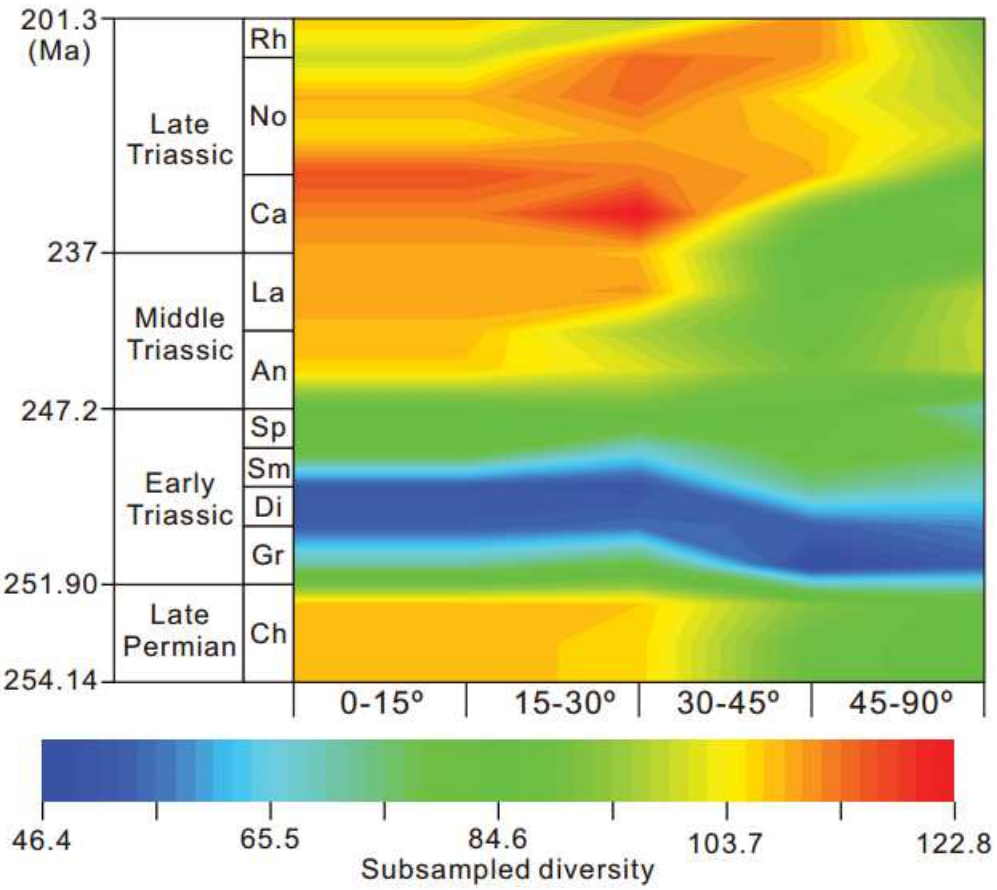

Fig. 2. Rarefied genus-level diversity trends related to latitude from the late Permian to the end Triassic. Data are standardized by repeatedly subsampling from a randomly generated set until a quota of 136 occurrences in each time bin at each latitudinal interval (*SI Appendix*, Table S3). Diversities are drawn as a contour map by using Origin Pro 2017 software. Ch, Changhsingian; Gr, Griesbachian; Di, Dienerian; Sm, Smithian; Sp, Spathian; An, Anisian; La, Ladinian; Ca, Carnian; No, Norian; Rh, Rhaetian.

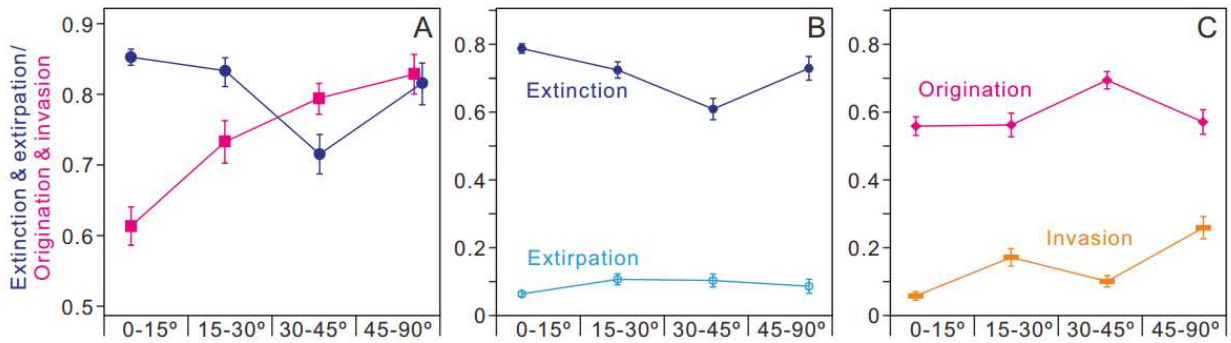

503

504 **Fig. 3.** Extinction and extirpation magnitudes in the Changhsingian and early Griesbachian

505 interval and origination and invasion magnitudes in the late Griesbachian-Smithian interval. (*A*)

506 The combined rates of extinction-extirpation and origination-invasion. (*B*) Extinction and

507 extirpation rates in the Changhsingian and early Griesbachian interval. (*C*) Origination and

508 invasion rates in the late Griesbachian-Smithian interval. Vertical bars represent standard errors.

509

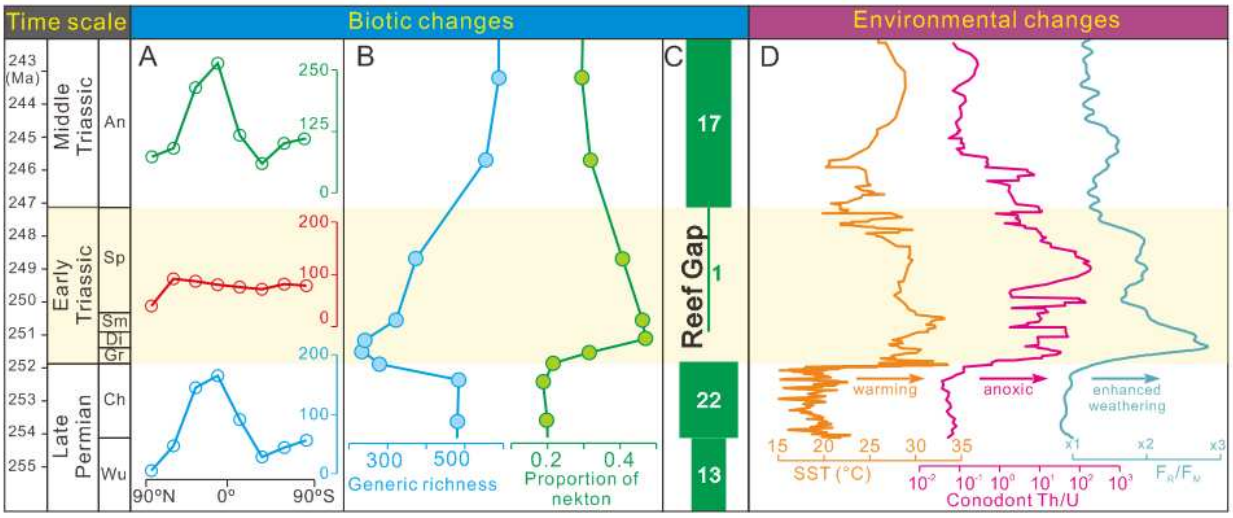

Fig. 4. Biotic and environmental changes throughout the late Permian to the Middle Triassic. (*A*) SQS diversities across latitudinal zones. (*B*) Genus richness and proportion of nekton (23). (*C*) The number of sites yielding metazoan reefs (50). (*D*) Sea surface temperature (SST), ocean redox, and continental weathering. SST values are derived from conodont oxygen isotope data (*SI Appendix*, Table S6, Database S2). Redox states of seawater are from conodont Th/U ratios (20). Riverine to mantle Sr flux ratios (F_R/F_M) calculated from conodont Sr isotopes reflect continental weathering change (43).